

# Nonequilibrium Green function modelling of transport in mesoscopic systems\*

Antti-Pekka Jauho  
*Mikroelektronik Centret*  
*Technical University of Denmark,*  
*Bldg. 345 East, Ørsted Plads,*  
*DK-2800 Kgs. Lyngby, Denmark*  
*E-mail: antti@mic.dtu.dk*

A generalized Landauer formula, derived with the methods due to Keldysh, and Baym and Kadanoff, is gaining widespread use in the modeling of transport in a large number of different mesoscopic systems. We review some of the recent developments, including transport in semiconductor superlattices, calculation of noise, and nanoelectromechanical systems.

## I. INTRODUCTION

### A. Some background, and a few historical remarks

A mesoscopic transport measurement is often concerned with a situation where the "device", whose properties are the subject of the investigation, is connected to structureless "contacts" via "ideal leads", i.e., in a situation which is accessible via the Landauer formula (or, more generally, the scattering approach to transport). An important feature is the fact that the size of the device is finite, and comparable to other important length-scales of the system, such as the phase-braking length or impurity mean free path. Thus the wave-properties of the charge carriers are important, leading to a number of interesting interference effects, such as weak localization, or universal conductance fluctuations. The conductance  $g$  of the device, for example, is then given by the celebrated Landauer formula[1, 2]

$$g = \frac{2e^2}{\hbar} |t|^2, \quad (1)$$

where  $t$  is the quantum mechanical transmission amplitude through the device.

The expression given above holds for the one-channel case, for low applied voltages, and in a situation when the "device" can be modelled by a noninteracting system. It is then natural to ask: Can this equation be generalized to the case, when interactions are important? Or: Can this equation be extended to time-dependent situations, or situations where superconductivity or magnetism are essential for the physics? How about strong driving fields?

Many authors have addressed these questions, with a number of different approaches. In the spirit of this conference, this review is concerned with the subset of these theories which use the nonequilibrium Green function technique. The earliest applications to mesoscopic transport, to my knowledge, are due to French researchers[3–6]: these researchers were mainly interested in inelastic effects in tunneling through oxide barriers. It is a curious side-note to observe that these early, and pioneering, papers were essentially forgotten during the 80's, but have obtained a substantial revival since mid-90's, and are presently cited more often than ever earlier. The explanation lies perhaps in the fact that the whole idea of mesoscopics is newer than these early papers, and it took the mesoscopic community a few years to realize the applicability of these ideas.

For the purposes of the present review, the next important development was the paper by Meir and Wingreen[7], which gave a very useful formal expression for the current in terms of the *exact* Green function of the device (or "central region"). This formula, and similar expressions obtained by other groups, were then applied to the Kondo problem out of equilibrium, a notoriously difficult problem, which remains a topic of active research even today. My previous review[8] in the first meeting of the present series focused in some of these issues, paying particular attention to the time-dependent generalization of the Meir-Wingreen expression[9]. I shall not repeat any of that material, but rather focus on other topics: the selection criterion has been that either they were not discussed during the first meeting, or that they are strictly post-1999 vintage. I have chosen to discuss three examples: (i) Transport in a semiconductor superlattice; (ii) Calculation of the noise in a spintronic system; and (iii) Tunneling transport in a nanoelectromechanical (NEMS) device. These three topics have a common feature: they all have practical applications, and, dare I say in the present meeting, even commercial potential.

It should be noted that there are many other recent applications of the NGF to mesoscopic transport which, due to space and time limitations, the present review does not address. One such example is transport in nanowires,

---

\* Based on a talk presented at the conference "Progress in Nonequilibrium Green Functions, Dresden, Germany, 19.-22. August 2002"

fabricated either with scanning tunnelling microscope, or with break junctions, which is a large research field where many theoretical calculations employ the NGF techniques. An exhaustive review has recently become available[10]. Molecular electronics holds enormous potential, and here a combination of *ab initio* electronic structure calculations (within the density-functional scheme) and NGF appears to be the most promising theoretical technique[11, 12]. Yet another example is the "circuit theory" developed by Nazarov[13, 14], which has successfully been applied to a number of hybrid structures, consisting of superconductors, ferromagnets, or semiconductors. The more abstract field-theoretic formulations, based on path-integrals and/or Grassmann variables fall also outside our present purposes, even though they play an important role in the study of disordered systems, or dephasing due to the environment.

### B. The basic equations, and their limitations

For completeness, we sketch here a derivation of the basic expressions used in the theory. Several more complete accounts are available elsewhere[8, 9, 15]. A brief reminder of how the nonequilibrium formalism works in the context of mesoscopic transport measurements is also in place. One reason is as follows. In the remote past the contacts and the central region (i.e., the "device") are assumed to be decoupled, and each region is in thermal equilibrium. The equilibrium distribution functions for the three regions are characterized by their respective chemical potentials; these do not have to coincide nor are the differences between the chemical potentials necessarily small. The couplings between the different regions are then established and treated as perturbations via the standard techniques of perturbation theory. The nonequilibrium nature of the problem manifests itself in that symmetry of remote past and remote future has been broken, and thus one must do the calculations on the two-branch time contour. It is important to notice that the couplings do not have to be small, e.g., with respect to spacings or  $k_B T$ , and typically must be treated to all orders.

Let us next consider some generic Hamiltonians:  $H = H_L + H_R + H_T + H_{\text{cen}}$ , or, explicitly:

$$H = \sum_{k,\alpha \in L/R} \epsilon_{k,\alpha} c_{k,\alpha}^\dagger c_{k,\alpha} + \sum_{k,\alpha \in L/R; n} \left[ V_{k\alpha;n} c_{k,\alpha}^\dagger d_n + \text{h.c.} \right] + H_{\text{cen}} [\{d_n\}, \{d_n^\dagger\}] , \quad (2)$$

where the central part Hamiltonian must be chosen according to the system under consideration. The operators  $\{d_n\}, \{d_n^\dagger\}$  refer to a complete set of single-particle states of the central region. Occasionally we specify explicitly the orbital and spin quantum numbers:  $n = m, \sigma$ , and analogously for the states in the leads. The derivation of the basic formula for the current does not require an explicit form for  $H_{\text{cen}}$ ; the actual evaluation of the formula of course requires this information. We write  $H_{\text{cen}} = \sum_n \epsilon_n d_n^\dagger d_n + H_{\text{int}}$ , where  $H_{\text{int}}$  could be electron-phonon interaction,

$$H_{\text{int}}^{\text{el-ph}} = \sum_{m\sigma} d_{m,\sigma}^\dagger d_{m,\sigma} \sum_{\mathbf{q}} M_{m,\mathbf{q}} [a_{\mathbf{q}}^\dagger + a_{\mathbf{q}}] , \quad (3)$$

or an Anderson impurity:

$$H_{\text{int}}^A = U \sum_m d_{m,\uparrow}^\dagger d_{m,\uparrow} d_{m,\downarrow}^\dagger d_{m,\downarrow} . \quad (4)$$

The current operator for the (say) left lead is

$$I_L = -e \dot{N}_L = -\frac{ie}{\hbar} [H, N_L] = -\frac{ie}{\hbar} \sum_{k,n} \left[ -V_{kL;n} c_{kL}^\dagger d_n + V_{kL;n}^* d_n^\dagger c_{kL} \right] . \quad (5)$$

The physically relevant observables can be expressed in terms of expectation values of the current operator, or its higher powers. For example, one can show[9, 15] that the current leaving the left contact is

$$\langle I_L \rangle = J_L(t) = -\frac{2e}{\hbar} \int_{-\infty}^t dt_1 \int \frac{d\epsilon}{2\pi} \text{ImTr} \left\{ e^{-i\epsilon(t_1-t)} \Gamma^L(\epsilon, t_1, t) \times [\mathbf{G}^<(t, t_1) + f_L^0(\epsilon) \mathbf{G}^r(t, t_1)] \right\} . \quad (6)$$

Here the Green functions are defined by

$$G_{nm}^<(t, t_1) = i\langle d_m^\dagger(t_1)d_n(t) \rangle \quad (7)$$

$$G_{nm}^r(t, t_1) = -i\theta(t - t_1)\langle [d_n(t), d_m^\dagger(t_1)] \rangle, \quad (8)$$

$\Gamma_{mn}$  describes the coupling between the central region and the contacts, and  $f_L^0(\epsilon)$  is the equilibrium distribution function of the left contact. In the dc-limit, (6) reduces to the result of Meir and Wingreen[7]:

$$\begin{aligned} J &= \frac{ie}{2\hbar} \int \frac{d\epsilon}{2\pi} \text{Tr} \left\{ [\Gamma^L(\epsilon) - \Gamma^R(\epsilon)] \mathbf{G}^<(\epsilon) \right. \\ &\quad \left. + [f_L^0(\epsilon)\Gamma^L(\epsilon) - f_R^0(\epsilon)\Gamma^R(\epsilon)] [\mathbf{G}^r(\epsilon) - \mathbf{G}^a(\epsilon)] \right\} \end{aligned} \quad (9)$$

$$= \frac{ie}{\hbar} \int \frac{d\epsilon}{2\pi} [f_L(\epsilon) - f_R(\epsilon)] T(\epsilon), \quad (10)$$

where

$$T(\epsilon) = \text{Tr} \left\{ \frac{\Gamma^L(\epsilon)\Gamma^R(\epsilon)}{\Gamma^L(\epsilon) + \Gamma^R(\epsilon)} [\mathbf{G}^r(\epsilon) - \mathbf{G}^a(\epsilon)] \right\}. \quad (11)$$

The expressions (6) and (10) are the central formal results whose consequences we explore in this review.[53] They are formally exact, and give the *tunneling* current for an interacting system coupled to noninteracting contacts (or, more precisely, for contacts which can be described by an effective single-body Hamiltonian). Thus, in a time-dependent situation the displacement current must be considered separately. It should also be noted that these equations only *define* the starting point of any calculation: to get into physical results one must evaluate the correlation function and the retarded/advanced Green function, Eqs.(7) and (8), respectively. These functions obey the Keldysh equation, and the (nonequilibrium) Dyson equation:

$$G^< = G^r \Sigma^< G^a, \quad (12)$$

$$G^r = G_0^r + G_0^r \Sigma^r G^r. \quad (13)$$

The success of the theory depends on whether one can construct a self-energy functional that captures the essential physics, and that a good solution can be found for these coupled equations. Both of these steps may be hard indeed.

## II. TRANSPORT IN A SEMICONDUCTOR SUPERLATTICE

In 1970 Esaki and Tsu[16] suggested that semiconductor superlattices, man-made structures which consist of alternating layers of different semiconductor materials, would have physical properties which could be used for a number of device applications. Very shortly, the spatial variations in the band-gaps will lead to a spatially varying conduction band edge, which supports minibands, which in turn display very interesting transport properties, such as Bloch oscillations, or negative differential resistance. A well known-result is the Esaki-Tsu IV-characteristic,

$$I(V) = 2I_{\max} V_0 \frac{V}{V^2 + V_0^2}, \quad (14)$$

where  $I_{\max}$  and  $V_0$  depend on the physical parameters of the system, such as the superlattice period, scattering rate, and temperature. To derive expressions like this, three main approaches have been used in the literature: (i) Miniband transport[16], (ii) Wannier-Stark hopping[17], and (iii) sequential tunneling[18]. The three different approaches have different domains of validity, and are all likely to fail if the three basic energy scales, i.e. scattering induced broadening, miniband width, and potential drop per period all have comparable values. The basic features of these three approaches are summarized in Figure 1.

In order to map out the boundaries of the various domains of validity, and to access the region where the approaches (i)–(iii) fail, a higher level theory is required. To achieve this, Andreas Wacker and myself, together with several colleagues, launched a program whose task was to develop a nonequilibrium Green function theory for superlattice transport.[54] Certain aspects of this program are now completed[22, 23], and in what follows I will review some of the highlights. It should be noted that the literature on superlattice transport is vast and here I can give only a

TABLE I: The three standard approaches to miniband transport, and the physical picture underlying them.(Courtesy of A. Wacker.)

	coupling $T_1$	field drop $eFd$	scattering $\Gamma$
Miniband conduction	exact miniband	acceleration	golden rule
Wannier Stark hopping	exact: Wannier Stark states		golden rule
Sequential tunneling	lowest order	energy mismatch	”exact” spectral function

very superficial discussion; the reader is referred to two recent review articles where a much fuller account can be found[24, 25].

Let me start with a few disclaimers. The quantum theory has *not* yet been fully developed to the case when the electric field is inhomogeneous (domain formation), nor is it available for the time-dependent case (photo-assisted transport; progress is however being made see, *e.g.*, Appendix C in the review by Wacker[24]). For these important situations one has to apply one of the simpler approaches discussed above. As far scattering is concerned, impurity scattering and phonon scattering have been discussed, but carrier-carrier interaction is still a future task.

The task is now to solve the coupled Keldysh and Dyson equations, Eq.(12–13). We adopt the tight-binding representation of the single-particle Hamiltonian:

$$H_{n,m} = (\delta_{nm-1} + \delta_{n,m+1})T_1 + \delta_{n,m}(E_k - neFd), \quad (15)$$

where  $T_1$  is the nearest neighbor coupling,  $E_k = \hbar^2 k^2 / (2m)$  the kinetic energy perpendicular to the growth direction,  $F$  the applied field, and  $d$  the superlattice period. In this basis the Keldysh and Dyson equations (12–13) read

$$\begin{aligned} G_{mn}^<(E) &= \sum_{m_1} G_{mm_1}^r \left( E + eFd \frac{m_1 - n}{2} \right) \\ &\times \Sigma_{m_1}^< \left[ E + eFd \left( m_1 - \frac{m+n}{2} \right) \right] \\ &\times G_{m_1 n}^a \left( E + eFd \frac{m_1 - m}{2} \right) \end{aligned} \quad (16)$$

$$\begin{aligned} G_{mn}^r(E) &= g_m^r \left( E + eFd \frac{m - n}{2} \right) \\ &\times \left[ \delta_{mn} + \sum_l \Sigma_{ml}^r \left( E + eFd \frac{l - n}{2} \right) \right. \\ &\times \left. G_{ln}^r \left( E + eFd \frac{l - m}{2} \right) \right]. \end{aligned} \quad (17)$$

Next one needs to specify the self-energies. We have considered[22, 23] impurity scattering, optical phonon scattering, and mimicked acoustic phonon scattering by a very low-energy optical phonon, all in the self-consistent Born

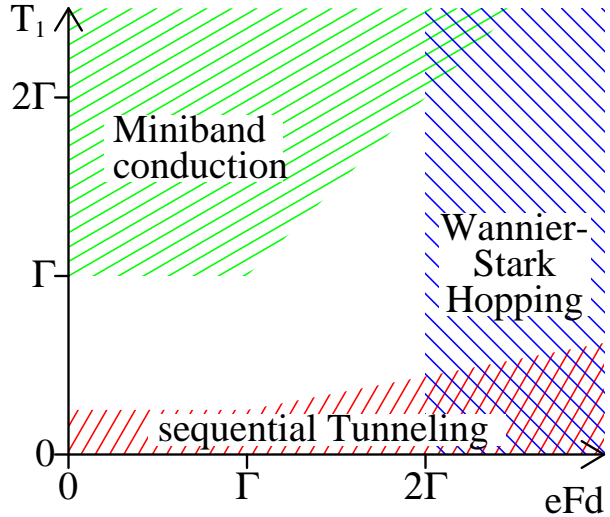


FIG. 1: The range of validity of various approaches to superlattice transport, in the parameter space spanned by the nearest-neighbor coupling  $T_1$ , and the potential energy drop  $eFd$  per period, in units of the scattering width  $\Gamma$ .

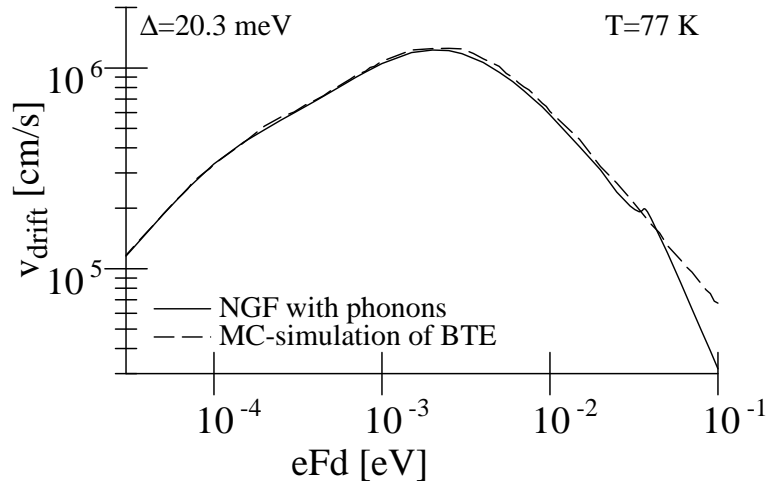


FIG. 2: Drift velocity vs. applied field.

approximation. By numerically solving these coupled equations, computing the current, and comparing to the corresponding IV-curves found by the simpler approaches (i)–(iii), we can construct a "phase-diagram" (see Figure 2), which indicates where the simpler approaches hold, and where a quantum approach is necessary.

We have also compared the quantum mechanical drift–velocity vs. field relation to the results obtained with a semiclassical Monte Carlo simulation. This is quite interesting because the two methods are totally different, and both require computationally rather intensive calculations. Typical results are shown in Figure 3. For the parameters considered here, the Monte Carlo simulation gives very good results, except that it misses the weak phonon replica seen in the quantum calculation.

The approach sketched here is ideally suited to transport phenomena where quantum phenomena, such as resonant tunneling, or phonon-assisted tunneling, play an important role. Another application concerns quantum cascade lasers[26], where the current injection occurs through a "funnel": the superlattice is designed so that the miniband width varies with distance. Another recent calculation concerns the evaluation of gain in such structures[27].

### III. NOISE IN SPINTRONICS

The emerging field of spintronics[28–30], where, in addition to the charge, also the electron spin is used to design new devices, has led to fascinating and novel ideas such as spin filters[31–33], spin field-effect transistors[34], and

proposals for solid state quantum computing[35]. For example, quantum dot systems can in principle be used to control the electron spin and are thus suitable for creating quantum bits relevant for quantum gate operations[36].

A detailed theoretical study of nonequilibrium transport properties of spintronic devices is necessary in order to understand the basic physical phenomena and to predict new functionalities. Calculation of the current, for example, can give the conductance/resistance of a system and its dependence on magnetic field, Coulomb interaction, spin-flip and so on. On the other hand, current fluctuations, due to the granularity of the charge (shot noise[37]), are also relevant because their measurements can provide additional information not contained in the average current[38].

Here we illustrate how the nonequilibrium Green function technique can be used to calculate current and its fluctuations (noise)[55] in a quantum dot coupled to two ferromagnetic leads as a function of the applied voltage for parallel (P) and antiparallel (AP) lead-polarization alignments. We include Coulomb interaction in the Hartree-Fock approximation as well as spin-flip in the dot. We show that spin-flip makes the alignment of the lead polarizations less important; both P and AP results coincide for large enough spin-flip rates. This fact gives rise to a reduction of both Fano factor[56] and tunnelling magnetoresistance (TMR) as we show below.

We model the central region with the Hamiltonian

$$H_D = \sum_{\sigma} \epsilon_0 d_{\sigma}^{\dagger} d_{\sigma} + U n_{\uparrow} n_{\downarrow} + R(d_{\uparrow}^{\dagger} d_{\downarrow} + d_{\downarrow}^{\dagger} d_{\uparrow}), \quad (18)$$

where  $d_{\sigma}$  ( $d_{\sigma}^{\dagger}$ ) destroys (creates) an electron in the dot with spin  $\sigma$  and the energy  $\epsilon_0$  is spin independent[43, 44]. In addition, we assume that the dot is a small enough in order to have only one active level  $\epsilon_0$ . In the presence of a voltage the level shifts by  $\epsilon_0 = \epsilon_d - \frac{eV}{2}$ , where  $\epsilon_d$  is the dot level for zero bias. In a more realistic calculation one should determine the bias dependence self-consistently. The spin-flip scattering amplitude  $R$  is viewed here as a phenomenological parameter. The spin-flip process lifts the degeneracy, splitting the quantum dot level to two states, let us call them  $\epsilon_{1,2}$ , with corresponding operators. The current is readily evaluated with the formulas given in Section 1.2 with the result

$$J_L = \frac{2e}{\hbar} \text{Re} \int dt_2 \text{Tr}\{\mathbf{G}^r(t, t_2) \Sigma^{L<} (t_2, t) + \mathbf{G}^{<} (t, t_2) \Sigma^{L a} (t_2, t)\}, \quad (19)$$

where  $\mathbf{G}^r$  and  $\mathbf{G}^{<}$  are the nonequilibrium dot Green functions, with elements  $G_{ij}^{<} (t, t_2) = i \langle d_j^{\dagger}(t_2) d_i(t) \rangle$  and  $G_{ij}^r (t, t_2) = -i \theta(t - t_2) \langle \{d_i(t), d_j^{\dagger}(t_2)\} \rangle$ . The lesser (retarded, advanced) tunnelling self-energy is given by

$$\begin{aligned} \Sigma^{L<(r,a)} (t_2, t) &= \frac{1}{2} \sum_k |t_{kL}^2| \\ &\times \begin{pmatrix} g_{kL\uparrow}^{<(r,a)}(t_2, t) + g_{kL\downarrow}^{<(r,a)}(t_2, t) & g_{kL\uparrow}^{<(r,a)}(t_2, t) - g_{kL\downarrow}^{<(r,a)}(t_2, t) \\ g_{kL\uparrow}^{<(r,a)}(t_2, t) - g_{kL\downarrow}^{<(r,a)}(t_2, t) & g_{kL\uparrow}^{<(r,a)}(t_2, t) + g_{kL\downarrow}^{<(r,a)}(t_2, t) \end{pmatrix}, \end{aligned} \quad (20)$$

where  $g_{kL\sigma}^{<(r,a)}$  is the lesser (retarded, advanced) uncoupled Green function for lead  $L$ . Equation (20) leads to a generalization of the coupling  $\Gamma$  found in Section 1.2 above; the coupling matrix now becomes

$$\Gamma^L = \frac{1}{2} \begin{pmatrix} \Gamma_{\uparrow}^L + \Gamma_{\downarrow}^L & \Gamma_{\uparrow}^L - \Gamma_{\downarrow}^L \\ \Gamma_{\uparrow}^L - \Gamma_{\downarrow}^L & \Gamma_{\uparrow}^L + \Gamma_{\downarrow}^L \end{pmatrix}. \quad (21)$$

Accounting for Coulomb interaction in the Hartree-Fock approximation, we can write down a matrix Dyson equation for the retarded Green function,  $\mathbf{G}^r = \mathbf{G}^{0r} + \mathbf{G}^{0r} \Sigma^r \mathbf{G}^r$ , and a Keldysh equation for the lesser Green function  $\mathbf{G}^{<} = \mathbf{G}^r \Sigma^{<} \mathbf{G}^a$ , where  $\mathbf{G}^{0r}$  is the uncoupled dot Green function. In these equations the self energies are the sum of the left and right self energies, i.e.,  $\Sigma^{(r,<)} = \Sigma^{L(r,<)} + \Sigma^{R(r,<)}$ . A self-consistent calculation is required to calculate  $\langle n_{\bar{i}} \rangle$  and  $\langle d_i^{\dagger} d_i \rangle$ , which are given by the lesser Green function,  $\langle d_j^{\dagger} d_i \rangle = \int \frac{d\omega}{2\pi} \text{Im} G_{ij}^{<}(\omega)$ .

The current operator can be written as its average value plus some fluctuation, i.e.,  $I_{\eta} = J_{\eta} + \delta I_{\eta}$  (here  $\eta = L/R$  labels the contacts). In our system there are two sources of noise, namely, thermal noise and shot noise. The first one is due to thermal fluctuations in the occupations of the leads. It vanishes for zero temperature, but can be finite for  $T \neq 0$  and  $eV = 0$ . On the other hand, shot noise is due to the granularity of the electron charge; it is a nonequilibrium property of the system in the sense that it is nonzero only when there is a finite current ( $eV \neq 0$ ). To calculate the noise (thermal+shot noise) we use the definition  $S_{\eta\eta'}(t - t') = \langle \{\delta I_{\eta}(t), \delta I_{\eta'}(t')\} \rangle$ , which can also be written as  $S_{\eta\eta'}(t - t') = \langle \{I_{\eta}(t), I_{\eta'}(t')\} \rangle - 2J_{\eta}^2$ . After a lengthy but straightforward calculation[45], we find for the noise power spectrum (*dc* limit; a scalar version of this equation has been found earlier[42])

$$\begin{aligned}
S_{\eta\eta'}(0) = \frac{e^2}{\hbar} \int \frac{d\omega}{2\pi} \{ & \delta_{\eta\eta'} i n_\eta \Gamma^\eta \mathbf{G}^> - \delta_{\eta\eta'} i (1 - n_\eta) \Gamma^\eta \mathbf{G}^< + \mathbf{G}^< \Gamma^\eta \mathbf{G}^> \Gamma^{\eta'} \\
& - n_\eta (1 - n_{\eta'}) \mathbf{G}^r \Gamma^\eta \mathbf{G}^r \Gamma^{\eta'} - n_{\eta'} (1 - n_\eta) \mathbf{G}^a \Gamma^\eta \mathbf{G}^a \Gamma^{\eta'} \\
& - \mathbf{G}^< \Gamma^\eta [(1 - n_{\eta'}) \mathbf{G}^r - (1 - n_\eta) \mathbf{G}^a] \Gamma^{\eta'} \\
& + (n_\eta \mathbf{G}^r - n_{\eta'} \mathbf{G}^a) \Gamma^\eta \mathbf{G}^> \Gamma^{\eta'} \}.
\end{aligned} \tag{22}$$

The *dc* noise (zero frequency) is position independent, and it is possible to show that  $S_{LL}(0) = S_{RR}(0) = -S_{LR}(0) = -S_{RL}(0)$ [37]. In our numerics we make a few simplifying assumptions. We assume that the couplings  $\Gamma^\eta$  are energy independent, but allow a polarization dependence. For the physical parameters we use accepted values from the current literature[43]. Our Hartree-Fock approximation for the electron-electron interaction does not include correlations of the Kondo type, however we do not expect these to change our results in the present range of parameters.

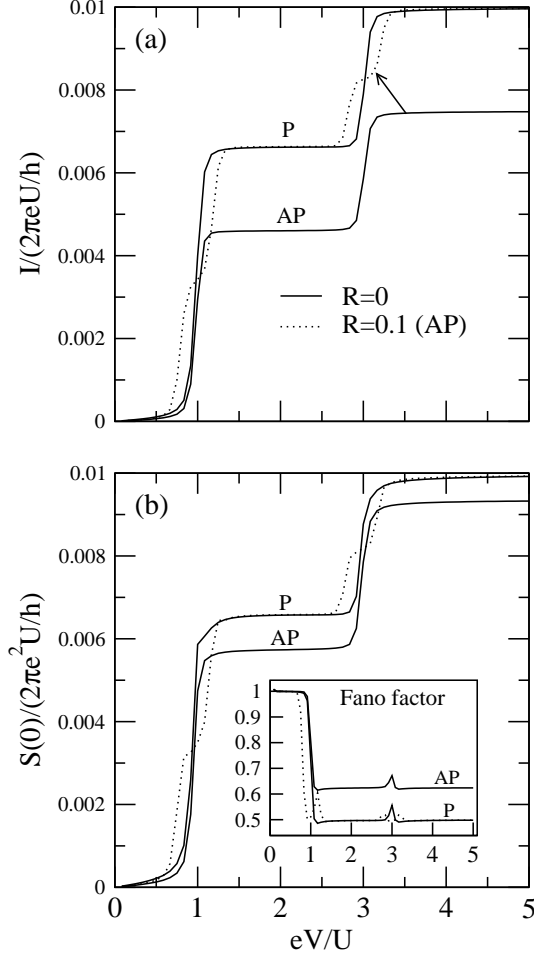


FIG. 3: Current and noise as a function of the bias for parallel (P) and antiparallel (AP) alignments and with  $R = 0$  and  $0.1U$ . The curves for  $R = 0.1U$  are only for the AP alignment; observe that these are almost on top of the P curves, except within the sloping region around  $U$  and  $3U$ . Both current and noise are reduced when the right lead changes its polarization from P to AP, following the typical behavior of TMR. The inset shows a suppression of the AP-Fano factor due to spin-flip.

Figure 4 shows current (a) and noise (b) as a function of the bias with  $R = 0$  (solid line) and  $R = 0.1U$  (dotted line) for both P and AP configurations. Because P and AP curves for  $R = 0.1U$  coincide, we plotted only the AP case. The first enhancement of the current and noise at  $eV = U$  happens when  $\epsilon_0$  crosses the left chemical potential, allowing electrons to tunnel from the emitter (left lead) to the dot and then to the collector (right lead). The current and noise

remain constant until the second level  $\epsilon_0 + U$  reaches  $\mu_L$  at  $eV = 3U$ , when another enhancement is observed. Each enhancement corresponds to a peak in the differential conductance  $\sigma_{\text{diff}}$ . When the system changes from parallel (P) to antiparallel (AP) configurations the current is reduced. This is a typical behavior of tunnelling magnetoresistance (TMR). The noise is also affected by this resistance variation, showing a similar reduction.

Looking at the effects of spin-flip on current and noise we see that the AP curves with  $R = 0.1U$  (dotted lines) tend to lie on the P curves with  $R = 0$ , thus showing that lead alignments are less important when spin-flip plays a part. This AP current enhancement due to spin-flip gives rise to a reduction of the TMR; since  $\text{TMR} = (I_P - I_{AP})/I_{AP}$ , when  $I_{AP} \rightarrow I_P$  we have  $\text{TMR} \rightarrow 0$ . For a somewhat simpler model W. Rudziński *et al.*[43] found a similar behavior.

#### IV. NANOELECTROMECHANICAL SYSTEMS

Microelectromechanical systems (MEMS) are today an important part of our technology. Their functionality is based on combining mechanical and electronic degrees of freedom, the great advantage being that the whole device can be fabricated with standard Si-processing technology. Typical applications include hearing aids, sensors, or actuators. As the fabrication technology gets refined, we soon expect to find systems where the mechanical parts are in the nanometer range, see the review by Craighead[47]; hence the acronym NEMS. An example is the nanomechanical electron shuttle constructed by Erbe *et al.*[48] (see Figure 5), based on the theoretical ideas of Gorelik *et al.*[49] Transport through the device was modelled with rate-equations[48], however these are not expected to work when one

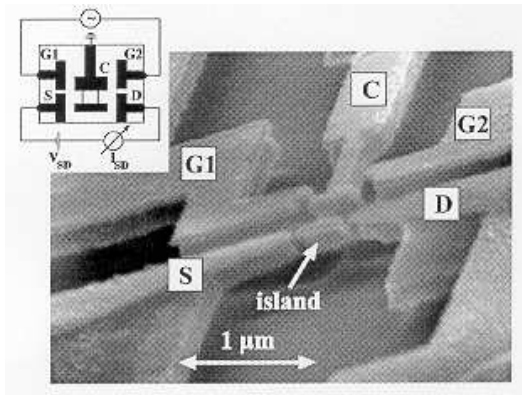


FIG. 4: The nanomechanical electron shuttle. An ac-voltage coupled to the gates  $G_1$  and  $G_2$  causes the central electrode, the "clapper",  $C$  to oscillate, and charges tunnel from the source  $S$  to the island, and from the island to the drain  $D$ .

enters the coherent transport regime, at lower temperatures and smaller devices, and a quantum theory of transport must be invoked. Such an approach has recently been formulated by Fedorets *et al.*[50], and I'll give a brief introduction to this topic.

The archetypal NEMS device consists of a moving part, and electrodes. We shall model the moving part by a quantum well, whose coupling to the electrodes are position dependent: the tunnelling amplitude is written as  $T_{L/R}(x(t)) = \tau_{L/R} \exp[\mp x(t)/\lambda]$ , where  $\lambda$  is some characteristic tunnelling length, and  $x(t)$  is the center-of-mass coordinate of the moving quantum dot. The electronic degrees of freedom are governed by exactly the same Hamiltonians as discussed in Section 2; now the dot-level depends on the dot's location via  $\epsilon_d = \epsilon_0 - Ex(t)$ , where  $E$  is the electric field, which depends on the applied bias.[57] The center-of-mass of the dot obeys Newton's equation of motion,

$$\ddot{x} + \omega_0^2 x = F(x)/M, \quad (23)$$

where  $M$  is the mass of the grain,  $\omega_0^2 = k/M$  is the characteristic frequency, and  $F$  is the force, which includes both the electric force acting on the charge(s) on the dot, and an exchange force, which arises due to the  $x$ -dependence of the tunnelling matrix elements. One can evaluate the force via  $F = -\langle \partial H / \partial x \rangle$ , and the result is

$$F(t) = -iEG^<(t, t) + 2/\lambda \sum_{\alpha, k} (-1)^\alpha T_\alpha(t) \text{Im}[G_{\alpha, k}^<(t, t)], \quad (24)$$

using the notation of Section 2. The problem is thus (again) reduced to the determination of the two lesser Green function:  $G^<$  for the dot, and the non-diagonal  $G_{\alpha, k}^< = i\langle c_{k, \alpha}^\dagger d(t) \rangle$ . Fedorets *et al.*[50] calculate these for a noninteracting system, and proceed to present an analysis of the mechanical stability of the system: does the dot execute

regular oscillations (whose frequencies are determined by an appropriate linearization of (23) and (24), or does it perhaps become unstable, as the bias is increased? The details of the analysis are not our concern here; the upshot is that above a certain threshold value an instability results. The analysis has also bearing on a recent experiment[51], where vibronic anomalies were observed in a single-C<sub>60</sub>-transistor when current was passed through it.

The analysis of Fedorets *et al.*[50] is very interesting and suggests for several further refinements. For example, what are the results for an interacting system (Coulomb blockade)? How about the environmental degrees of freedom? This issue was addressed recently Armour and MacKinnon[52], in a slightly different context. Finally, is it possible to combine the spintronic effects with charge shuttles? Can one envisage a spin shuttle? Will there be a new technology called NEMSS (nanoelectromechanical spin systems)?

## V. CONCLUSIONS

I have reviewed some of the post-1999 developments in applying NGF to modelling of transport in mesoscopic systems. The common theme in my review has been to focus on "real devices", which may have "real applications". I find it very pleasing that the NGF technique, often regarded as an academic exercise most suited for theoretical games, is now becoming a strong tool in the analysis of practical devices. This trend is also confirmed by several other talks at this conference. At the same time there is still much room for theoretical refinements, and I'm convinced that in the coming years we will witness significant progress in this field, both abstract and practical.

### Acknowledgments

The author is grateful to acknowledge fruitful collaborations with A. Wacker, and F. Macedo and J. C. Egues, which resulted in the material presented in Sections 2 and 3, respectively.

---

[1] R. Landauer, IBM J. Res. Dev. **1**, 233 (1957).  
[2] R. Landauer, Philos. Mag. **21**, 863 (1970).  
[3] C. Caroli, R. Combescot, D. Lederer, P. Nozieres, and D. Saint-James, J. Phys. C **4**, 2598 (1971).  
[4] C. Caroli, R. Combescot, P. Nozieres, and D. Saint-James, J. Phys. C **4**, 916 (1971).  
[5] C. Caroli, R. Combescot, P. Nozieres, and D. Saint-James, J. Phys. C **5**, 21 (1972).  
[6] R. Combescot, J. Phys. C **4**, 2611 (1971).  
[7] Y. Meir and N. S. Wingreen, Phys. Rev. Lett. **68**, 2512 (1992).  
[8] A. P. Jauho, pp. 250 – 273, in "Progress in Nonequilibrium Green's Functions", Ed. M. Bonitz, World Scientific, Singapore (2000).  
[9] A. P. Jauho, N. S. Wingreen, and Y. Meir, Phys. Rev. B **50**, 5528 (1994).  
[10] N. Agrait, A. Levy Yeyati, and J. M. van Ruitenbeek, to appear in Physics Reports (2002), archived at cond-mat/0208239.  
[11] M. Paulsson, F. Zahid, and S. Datta, to appear in "Nanoscience, Engineering and Technology Handbook", Eds. W. W. Goddard, D. Brenner, S. Lyshevski, and G. Iafrate, CRC Press (2002), archived at cond-mat/0208183.  
[12] M. Brandbyge, J. L. Mozos, P. Ordejón, J. Taylor, and K. Stokbro, Phys. Rev. B **65**, 165401 (2002).  
[13] Yu. V. Nazarov, Phys. Rev. Lett. **73**, 1420 (1994).  
[14] Yu. V. Nazarov, Superlattices Microstruct. **25**, 1221 (1999).  
[15] H. Haug and A. P. Jauho, *Quantum Kinetics in Transport and Optics of Semiconductors* (Springer Series in Solid-State Sciences, Vol. 123, Springer-Verlag, Berlin Heidelberg, 1996).  
[16] L. Esaki and R. Tsu, IBM J. Res. Develop. **14**, 61 (1970).  
[17] R. Tsu and G. Döhler, Phys. Rev. B **12**, 680 (1975).  
[18] D. Miller and B. Laikhtman, Phys. Rev. B **50**, 18426 (1994).  
[19] T. Kuhn, pp. 173 – 214, in: E. Schöll (Ed.), "Theory of Transport Properties of Semiconductor Nanostructures", Chapman & Hall, London, 1998.  
[20] V. V. Bryksin and P. Kleinert, J. Phys.: Condens. Matt. **9**, 15827 (1997).  
[21] X. L. Lei, N. J. M. Horing, and H. L. Cui, Phys. Rev. Lett. **66**, 3277 (1991).  
[22] A. Wacker and A. P. Jauho, Phys. Rev. Lett. **80**, 369 (1998).  
[23] A. Wacker, A. P. Jauho, S. Rott, A. Markus, P. Binder, and G. H. Döhler, Phys. Rev. Lett. **83**, 836 (1999).  
[24] A. Wacker, Phys. Rep. **357**, 1 (2002).  
[25] L. L. Bonilla, J. Phys.: Condens. Matt. **14**, R341 (2002).  
[26] J. Faist, F. Capasso, D. L. Sivco, C. Sirtori, A. L. Hutchinson, and A. Y. Cho, Science **24**, 553 (1994).  
[27] A. Wacker, to appear in Phys. Rev. B (2002).  
[28] D. D. Awschalom, M. E. Flatté and N. Samarth, Sci. Am. **286**(6), 66 (2002).

- [29] S. A. Wolf, D. D. Awschalom, R. A. Buhrman, J. M. Daughton, S. von Molnár, M. L. Roukes, A. Y. Chtchelkanova and D. M. Treger, *Science* **294**, 1488 (2001).
- [30] G. A. Prinz, *Science* **282**, 1660 (1998).
- [31] R. Fiederling, M. Keim, G. Reuscher, W. Ossau, G. Schmidt, A. Waag and L. W. Molenkamp, *Nature* **402**, 787 (1999).
- [32] J. C. Egues, *Phys. Rev. Lett.* **80**, 4578 (1998).
- [33] T. Koga, J. Nitta, H. Takayanagi and S. Datta, *Phys. Rev. Lett.* **88**, 126601 (2002).
- [34] S. Datta and B. Das, *Appl. Phys. Lett.* **56**, 665 (1990)
- [35] D. P. DiVincenzo, *Science* **270**, 255 (1995).
- [36] H. A. Engel, P. Recher and D. Loss, *Solid State Commun.* **119**, 229 (2001).
- [37] For a review on shot noise, see Ya. M. Blanter and M. Büttiker, *Phys. Rep.* **336**, 2 (2000).
- [38] For an example in the context of fractional charge, see C. L Kane and M. P. A. Fisher, *Nature* **389**, 119 (1997).
- [39] L. Y. Chen and C. S. Ting, *Phys. Rev. B* **43**, 4532 (1991).
- [40] S. Hershfield, *Phys. Rev. B* **46**, 7061 (1992).
- [41] G. H. Ding and T. K. Ng, *Phys. Rev. B* **56** 15521 (1997).
- [42] B. Dong and X. L. Lei, *J. Phys.: Condens. Matt.* **14**, 4963 (2002).
- [43] W. Rudziński and J. Barnaś, *Phys. Rev. B* **64**, 085318 (2001)
- [44] P. Zhang, Q. K. Xue and X. C. Xie, *cond-mat/0201465* (2002).
- [45] F. M. Souza, J. C. Egues and A. P. Jauho, in preparation.
- [46] R. Świrkowicz, J. Barnaś and M. Wilczyński, *J. Phys.: Condens. Matt.* **14**, 2011 (2002).
- [47] H. G. Craighead, *Science* **290**, 1532 (2000).
- [48] A. Erbe, C. Weiss, W. Zwerger, and R. H. Blick, *Phys. Rev. Lett.* **87**, 096106 (2001).
- [49] L. Y. Gorelik, A. Isacsson, M. B. Voinova, B. Kasemo, R. I. Shekhter, and M. Jonson, *Phys. Rev. Lett.* **80**, 4526 (1998).
- [50] D. Fedorets, L. Y. Gorlik, R. I. Shekhter, and M. Jonson, *Europhys. Lett.* **58**, 99 (2002).
- [51] H. Park, J. Park, A. K. L. Lim, E. H. Anderson, Alivistros A. P., and P. L. McEuen, *Nature* **407**, 58 (2000).
- [52] A. D. Armour and A. MacKinnon *Phys. Rev. B* **66**, 035333 (2002).
- [53] In the Section 3 we also give an analogous expression for the noise spectrum.
- [54] There are other theoretical methods capable of including (some) quantum effects, such as the density-matrix method[19, 20], or the balance equation approach.[21]
- [55] NGF calculations of noise have been performed by several groups[39–42].
- [56] The Fano factor, defined as  $\gamma = S(0)/2eI$ , characterizes deviations from the Poissonian noise.
- [57] In principle a rather complicated electrostatic calculation, including the screening due to all neighboring metallic bodies, is required.